Effects of contact metamorphism on the chemistry of calcareous rocks in the Big Horse Limestone Member, Notch Peak, Utah

Theodore C. Labotka

Department of Geological Sciences, University of Tennessee, Knoxville, Tennessee 37996, U.S.A.

Peter I. Nabelek

Department of Geology, University of Missouri, Columbia, Missouri 65211, U.S.A.

J. J. Papike

Institute for the Study of Mineral Deposits, South Dakota School of Mines and Technology, Rapid City, South Dakota 57701, U.S.A.

Victoria C. Hover-Granath

Conoco, Inc., Ponca City, Oklahoma 74603, U.S.A.

J. C. Laul

Radiological Sciences Department, Battelle Northwest, Richland, Washington 99352, U.S.A.

Abstract

The Jurassic Notch Peak stock intruded Upper Cambrian limestones and calcareous argillites of the Big Horse Limestone Member of the Orr Formation in west-central Utah. Previous petrologic and stable-isotope studies showed that the argillites interacted with more than two rock volumes of externally derived H_2O, whereas the limestones were impervious to the infiltrating fluid. Thirty-four major, minor, and trace elements were analyzed in argillites and limestones to determine whether the substantial influx of H_2O from the crystallizing pluton caused a change in the composition of the host rocks. The variability in the chemistry of the major elements is dominated by variability inherited from the protolith and by loss of CO_2. The limestone samples were essentially unaffected by metamorphism because they underwent a small amount of recrystallization. The argillite samples, however, were nearly completely decarbonated during metamorphism. The ranges in major-element composition were unaffected by the great loss of CO_2. There is no significant difference in the major-element chemistry with metamorphic grade, including the abundances of alkali elements. The variance in the major-element chemistry can be explained accurately by three sedimentary components: calcite, quartz + feldspar, and mica. The siliciclastic components were probably sorted independently in the sedimentary environment because of differences in grain shape. The abundances of all trace elements, except Sr, are strongly correlated with geochemically similar major elements. Sr shows very poor correlation with Ca in argillite samples and has enhanced abundances in some high-grade samples. The anomalous samples also contain high abundances of Ba, Rb, and K, and a cluster analysis groups Sr with these elements. The poor correlations among Sr and the other elements are caused by its dual affinity for alkali feldspar and calcite. The high abundance of feldspar in some high-grade samples indicates that feldspar components migrated over a volume of about 2 L during recrystallization of coarse-grained vesuvianite- and garnet-bearing samples. The results of the study indicate that there was no detectable, systematic change in composition with metamorphic grade. There is no evidence for large-scale migration of major or trace elements, despite the apparent substantial infiltration of H_2O during metamorphism.

Introduction

Metamorphism of sedimentary rocks is generally considered to be an isochemical process, except for the loss of CO_2 and H_2O. The loss of volatile components during metamorphism reflects the progressive equilibration of rocks with pore fluids generated by the rock or by infiltration from an external reservoir. Studies of the nature of the interaction between metasedimentary rocks and fluid in one stratigraphic unit in the contact-metamorphic aureole around the Notch Peak stock include petrologic (Hover-Granath et al., 1983), stable-isotope (Nabelek et al., 1984), fluid-inclusion (Feldman and Papike, 1981), and mass-balance (Labotka et al., 1988) techniques. In the mass-balance study by Labotka et al. (1988), the composition of the fluid expelled from the rock during meta-

morphism is calculated by balancing the mass transfer *protolith → metamorphic rock* for the volatile loss. The results are then compared with the equilibrium fluid composition to determine the amount of externally derived water that interacted with the rocks. The mass-balance calculation requires knowledge of whether the bulk compositions of the metamorphic rocks were altered by interaction with the fluid, other than loss of CO_2 and H_2O.

Changes in the bulk compositions of metamorphic rocks with grade have been studied in a few cases by Shaw (1956), Ferry (1982), and Labotka et al. (1984), who have found that metamorphism of pelitic rocks was isochemical, but calcic schists showed evidence for losses in Na and K and a change in the K/Na ratio at high grade (Ferry, 1982). The major-element chemistry controls the mineralogy of a rock, but many elements occur as minor or trace constituents in minerals. Trace-element abundances can be altered during metamorphism by exchange with an infiltrating fluid, even though the major-element chemistry remains invariant. Within the contact-metamorphic aureole around the Notch Peak stock, Utah, the interaction between fluid and rock was locally extensive—fluid/rock ratios in the argillaceous rocks were about 31 by mass. Here, the chemical variability of a single stratigraphic unit has been examined in detail to determine the effects of infiltration on the major- and trace-element composition of the host rock. The original impetus for this study was to use the contact-metamorphic aureole as a natural analogue to a disposal site for high-level radioactive wastes, to determine whether large-ion trace elements migrate during convective cooling over geologic time.

In the present study, the chemical variability is examined by a variety of statistical techniques to determine whether there was any discernible systematic change in composition during metamorphism. These methods must be used because *all* clastic sedimentary rocks, by the very nature of their origin, contain natural variability in bulk composition. The present study shows that the principal source of the compositional variability, for both major and trace elements, was mechanical mixing in the sedimentary environment. Metasomatic effects are indiscernible, and, if present, are minor and nonsystematic. The significance of this study is the isochemical nature of metamorphism and the justification of the mass-balance calculations to determine the amounts of CO_2 and H_2O released by the rocks.

GEOLOGY AND PETROLOGY OF THE BIG HORSE LIMESTONE MEMBER

The Notch Peak stock, located in west-central Utah, intruded the Weeks Formation and the Big Horse Limestone Member of the Orr Formation during Jurassic time (Fig. 1). The Notch Peak stock is composite, consisting of one granite and two quartz monzonite intrusions; the petrogenesis of the granitic rocks is described by Nabelek et al. (1986). The stock discordantly intrudes the gently

dipping Big Horse Limestone, which can be traced along strike for more than 6 km. The stratigraphy of the Big Horse Limestone Member has been described by Lohmann (1977) and consists of six upward-shallowing cycles deposited at the edge of the Late Cambrian platform. Each cycle consists of thinly interbedded calcareous mudstones and quartz-rich siltstones at its base. The proportion of carbonate increases upward within each cycle; the top is capped by algal or oolitic limestone, which contains a minor amount of siliceous clastic material. The individual cycles can be traced directly to the contact with the Notch Peak stock.

The petrology of the contact-metamorphosed Big Horse Limestone Member was described by Hover-Granath et al. (1983), who found a diversity of assemblages in the limestones and argillites. At low grades, the limestone marbles contain assemblages characterized by calcite + dolomite + talc and calcite + talc + tremolite. At medium grade, talc disappeared and diopside became stable. The highest-grade marbles contained forsterite in the assemblage. Although the marbles consist predominantly of calcite and dolomite, most samples contain low-variance assemblages; divariant assemblages in the system $CaO-MgO-SiO_2-H_2O-CO_2$ are common, and univariant assemblages occur. These assemblages indicate that the equilibrium values of P_{CO_2} and P_{H_2O} were buffered by the mineral reactions. In addition, the domains of equilibrium were found to be smaller than the area sampled by a thin section, indicating local control of μ_{CO_2} and μ_{H_2O} by the rock. At a pressure of 2 kbar, an estimate based on the amount of stratigraphic overburden during Jurassic time, the mineral assemblages appear to have buffered X_{CO_2} to values as high as 0.8 at temperatures as high as 575 °C.

The calcareous argillites were found by Hover-Granath et al. (1983) to contain assemblages radically different from those in the marbles. Unmetamorphosed argillites contain calcite + quartz + chlorite + muscovite. Phlogopite or K-feldspar is commonly present in addition. At low grades of metamorphism, these minerals reacted to form the assemblage calcite + quartz + diopside + K-feldspar. Some samples contain tremolite, and all contain calcic plagioclase. At high metamorphic grade, the argillites are characterized by the assemblage calcite + wollastonite + diopside + grossular + vesuvianite + K-feldspar + albite. Two isograds are shown on Figure 1 based on these assemblages. The lower-grade isograd is the first appearance of diopside. Rocks at lower grade than the diopside isograd are only incipiently metamorphosed or are unmetamorphosed. The higher-grade isograd marks the first appearance of wollastonite. Isograds based on reactions in the marbles are described by Hover-Granath et al. (1983).

The significant difference in assemblage between the argillites and marbles reflects not only the aluminous bulk composition of the argillites, but also the extremely H_2O-rich fluid phase in equilibrium with the argillites. The value of X_{CO_2} in the high-grade argillites was calculated
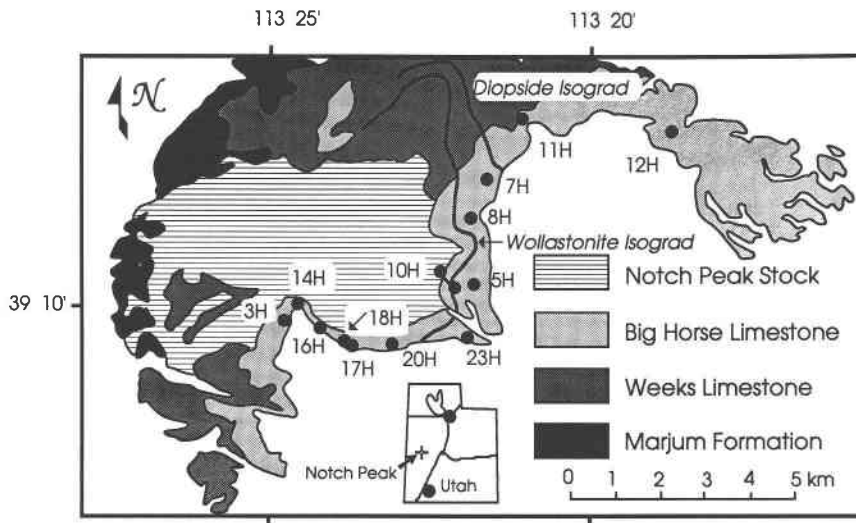
Fig. 1. Generalized geologic map, simplified from Hintze (1974), of the Notch Peak area, west-central Utah, showing the Jurassic Notch Peak stock, the Big Horse Limestone Member of the Orr Formation, and the underlying Weeks Formation, both of Late Cambrian age. Sample stations are shown as dots. At each station, samples were collected from cycles 1 and 2. The mineral assemblages are given in Table 1. The diopside and wollastonite isograds are also shown. These isograds are based on assemblages in the calcareous argillites and are dependent on the fluid-phase composition as well as the temperature. Calcite-rich marbles, which were in equilibrium with CO_2-rich fluids, may contain calcite + quartz within the wollastonite zone.

by Labotka et al. (1985) to be 0.008 ± 0.007. This low value appears to be the result of interaction with a large volume of water derived from the stock itself. O- and C-isotope systematics, determined by Nabelek et al. (1984), corroborate the infiltration by at least two rock volumes of H_2O that exchanged O with the argillites. The argillites had undergone fractional decarbonation, which dramatically reduced whole-rock $\delta^{13}C$ to values as low as -11.8, and whole rocks had exchanged O with a low-$\delta^{18}O$ fluid. Mass-balance calculations, based on the amount of CO_2 lost during metamorphism indicate that the mass of externally derived fluid was about 13 times the mass of the rock (Labotka et al., 1988). The interaction with this large mass was facilitated by a solid-volume loss of $23 \pm 7\%$ during decarbonation. A complete description of the interaction between the argillite and the infiltrating fluid is given by Labotka et al. (1988).

SAMPLES AND METHODS

Samples were collected from several stations, shown in Figure 1. At each locality, argillite samples were obtained from cycles 1 and 2, and marble samples were obtained from cycle 2. The cycles are numbered from the top; thus, the cycle 2 marble separates the two argillite layers. In addition, rocks from a short traverse from the contact with the stock at station 10H were collected. These samples came from the base of the Big Horse Limestone Member and were collected normal to the stratigraphic layering. Samples that were collected within the wollastonite zone are called high grade, those collected between the wollastonite and diopside isograds are called low grade, and those outside the diopside isograd are called unmetamorphosed. The resulting distribution of samples allows the testing of hypotheses regarding intrastratal and cross-stratal variances in chemistry over the entire range in metamorphic grade. The samples and their mineral assemblages are given in Table 1. There was a bias in sample collecting toward the high-grade rocks because of the interest in their petrogenesis. Thus there are only three sample sets for unmetamorphosed rocks. This lack of balance of sample size affects the analysis of variance, described below, but the sampling was sufficient to determine the relative importance of the various sources of chemical variance.

Bulk compositions of the samples were determined by X-ray fluorescence and instrumental neutron activation analysis (INAA). Si, Al, Ti, Fe, Mg, Mn, Ca, K, and P were analyzed by wavelength-dispersion X-ray fluorescence at the facilities of J. M. Rhodes at the University of Massachusetts using the method of Norrish and Hutton (1969). The precision is better than 40% for Mn and P, 10% for Mg, 5% for Ti, 3% for Fe and Ca, and 1% for Si, Al, and K. Na and trace elements were analyzed by INAA on 0.5 to 1.0 g of irradiated aliquots of ~5 kg of homogenized whole-rock powders. The gamma rays emitted from the samples were counted by Ge(Li) detectors using the sequential counting technique described by Laul (1979). Zn, Sb, Rb, Sr, and Zr data were obtained by coincidence/noncoincidence counting, which resulted in reduction of Compton background. Corrections were made for La, Ce, Nd, Sm, and Zr formed by fission of ^{235}U as a result of irradiation. U.S. Geological Survey standards GSP-1 and BHVO-1 and International Atomic Energy Agency standard Soil-5 were used to monitor the accuracy and precision of the results. The one-standard-deviation uncertainties on replicate standard and sample analyses are 1–2% for Na, Ce, Co, Sc, and Zn, 3% for Ba, Eu, Tb, and Rb, 4–5% for Sr, La, Sm, Yb, Lu, Hf, Ta, Th, U, and Cs, and <10% for Nd and Zr. The analyses are given in Table 2.

MAJOR-ELEMENT CHEMISTRY

Metamorphism is commonly considered to be isochemical, except for loss of volatiles. At Notch Peak, the

TABLE 1. Samples of the Big Horse Limestone Member of the Orr Formation

Sample	Distance from contact (m)*	Metamorphic grade**	Mineral assemblage†
		Cycle 1 argillites	
14H-80	72 ± 48	High	Cal + Wo + Di + Ves + Grs + Kfs + Pl
16H-84	120	High	Cal + Wo + Di + Ves + Grs + Kfs + Pl
3H-37	240	High	Cal + Wo + Di + Ves + Grs + Kfs + Pl
3H-36	240	High	Cal + Wo + Di + Grs + Kfs + Pl
18H-89	240	High	Cal + Wo + Di + Ves + Grs + Kfs
20H-98	360	High	Cal + Wo + Di + Grs + Kfs + Pl
5H-47	720	Low	Cal + Qtz + Tr + Di + Scp + Kfs
23H-137	720	Low	Cal + Qtz + Bt + Tr + Kfs + Pl
8H-129	960	Low	Cal + Qtz + Di + Grs + Scp + Kfs + Pl
7H-56	1440	Low	Cal + Qtz + Tr + Di + Kfs + Pl
11H-115	2400	Unmet.	Cal + Qtz + Ms + Bt + Pl
		Cycle 2 argillites	
16H-86	120	High	Cal + Wo + Di + Ves + Grs + Kfs + Pl
3H-40	204	High	Cal + Wo + Di + Ves
3H-39	240	High	Cal + Wo + Di + Ves + Kfs + Pl
17H-87	240	High	Cal + Wo + Di + Ves + Grs + Kfs + Pl
20H-100	360	High	Cal + Wo + Di + Ves + Pl
5H-44	720	Low	Cal + Qtz + Bt + Di + Kfs + Pl
23H-135	720	Low	Cal + Qtz + Bt + Tr + Di + Kfs + Pl
8H-59	960	Low	Cal + Bt + Di + Ves + Kfs + Pl
7H-54A	1440	Low	Cal + Qtz + Bt + Tr + Di + Scp + Kfs + Pl
11H-117	2400	Unmet.	Cal + Qtz + Ms + Kfs + Pl
12H-123	5280	Unmet.	Cal + Qtz + Ms + Bt + Kfs + Pl
		Cycle 2 limestones	
14H-81	72	High	Cal + Dol + Phl + Tr + Di + Fo
16H-85	120	High	Cal + Dol + Qtz + Tr + Chl + Pl
3H-38A	240	High	Cal + Dol + Qtz + Tr + Fo + Chl + Pl
18H-90	240	High	Cal + Dol + Qtz + Di + Chl + Kfs
20H-99	360	High	Cal + Dol + Qtz + Tlc + Tr + Pl
5H-46	720	Low	Cal + Dol + Qtz + Phl + Tlc + Tr + Chl + Pl
23H-136	720	Low	Cal + Qtz + Tlc + Tr + Chl + Pl
8H-130	960	Low	Cal + Qtz + Di + Kfs + Pl
7H-55	1440	Low	Cal + Dol + Qtz + Tlc + Tr + Scp
11H-116	2400	Unmet.	Cal + Dol + Phl + Chl + Pl
12H-122	5280	Unmet.	Cal + Dol + Qtz + Chl + Kfs + Pl
		10H traverse	
10H-102	1 ± 5	High	Cal + Qtz + Act + Di + Ves + Grs + Pl + Ep
10H-103	65	High	Cal + Wo + Di + Ves + Grs
10H-104	90	High	Cal + Qtz + Wo + Di + Ves + Grs + Kfs
10H-105	135	High	Cal + Wo + Di + Ves + Grs + Kfs + Pl
10H-106	435	High	Cal + Wo + Di + Ves + Grs + Kfs + Pl
10H-108	630	High	Cal + Wo + Di + Ves + Kfs + Pl
10H-107	735	Low	Cal + Dol + Tr + Di + Phl

* Map distance from contact. Error represents uncertainty in sample location.
** Grade represented by mineral assemblages in argillites. High = Wo zone. Low = Di zone.
† Complete mineral assemblages, including minor and trace minerals, are given in Hover-Granath et al. (1983). Mineral abbreviations are those of Kretz (1983).

loss of volatiles is dramatically illustrated by the argillites. Figure 2 shows the weight ratio of CO_2/CaO for the argillites, the limestone marble, and the short 10H traverse. In unmetamorphosed samples, essentially all the Ca occurs in calcite and dolomite. A decrease in the CO_2/CaO ratio with metamorphic grade represents progressive decarbonation. As seen in Figure 2, the marble samples have undergone little decarbonation; the CO_2/CaO ratio is nearly constant at 0.80 to 0.85 (the value for calcite is 0.79; dolomite has a value of 1.57). The unmetamorphosed argillites have CO_2/CaO values near that for calcite, but the value decreases to nearly 0.0 for the high-grade argillites. In many cases, e.g., the argillites from location 3H and 16H (Table 2), the decrease represents a loss of about 25 wt% CO_2 of unmetamorphosed sample. This great loss of CO_2 causes the apparent concentrations

of all remaining components to increase. Figure 3 illustrates the variation in K_2O and SiO_2, oxides representative of the silicate fraction, with metamorphic grade in argillites. There seems to be an increase in K_2O with grade, although some high-grade samples have low abundances of K_2O. This trend may represent a true increase in K_2O with grade, or may be an apparent increase as a result of loss of CO_2. SiO_2 appears to remain constant with grade, but SiO_2 may have been lost at high grades, with the apparent constancy resulting from loss of CO_2.

The volatile-loss effect on the concentrations can be eliminated by considering changes in the ratios of oxides. Clearly, the CO_2/CaO ratio illustrates the loss of CO_2. If Al_2O_3 is used as a reference, then systematic changes in oxide/Al_2O_3 ratios can indicate whether metasomatism had occurred. Figure 4 shows these ratios for TiO_2, K_2O,

TABLE 2A. Whole-rock analyses for cycle 1 argillites

Sample:	14H-80	16H-84	3H-37	3H-36	18H-89	20H-98	5H-47	23H-137	8H-129	7H-56	11H-115
SiO_2	55.90	53.20	46.20	55.50	37.60	58.50	28.50	33.40	53.50	40.30	21.50
TiO_2	0.61	0.58	0.61	0.66	0.31	0.66	0.40	0.52	0.61	0.41	0.14
Al_2O_3	9.50	7.80	9.80	11.00	4.60	9.20	7.20	8.00	12.30	6.30	2.20
Fe_2O_3	3.70	3.10	3.10	3.90	2.30	2.40	2.00	2.30	3.50	1.90	0.72
MnO	0.12	0.11	0.05	0.08	0.06	0.05	0.03	0.02	0.06	0.02	0.10
MgO	2.90	3.00	3.40	3.10	2.00	2.00	3.50	2.90	7.60	3.20	1.20
CaO	19.70	29.20	32.20	16.90	41.70	22.00	33.70	29.20	16.10	27.10	41.10
Na_2O	1.05	1.30	0.51	1.56	0.21	2.00	0.37	0.56	0.70	0.34	0.30
K_2O	4.90	1.74	1.72	5.52	0.78	3.89	1.93	2.48	4.02	1.66	0.62
P_2O_5	0.55	0.53	0.15	0.62	0.33	0.13	0.18	0.16	0.22	0.17	0.37
H_2O	0.15	0.11	0.26	0.18	0.15	0.09	0.16	0.25	0.51	0.18	0.27
CO_2	0.47	0.43	2.64	0.53	11.20	0.21	22.78	20.20	1.03	18.50	32.40
Total	99.55	101.10	100.64	99.55	101.24	101.13	100.75	99.99	100.15	100.08	100.92
					Trace elements (ppm)						
S	40	11	123	53	73	55	320	—	414	480	14
F	650	400	660	470	1800	240	770	—	1400	680	62
Cl	250	26	170	160	65	30	25	—	60	72	19
Cs	4.1	1.6	2.1	6.3	0.8	4.6	3.1	3.5	7.2	2.2	1.2
Rb	240	75	80	260	37	190	70	80	200	70	23
Ba	560	180	340	870	90	410	220	300	480	210	100
Pb	16	13	41	21	14	14	5	10	12	2	6
Sr	660	510	550	750	580	320	490	400	680	470	510
Cr	48	35	40	41	25	35	25	35	48	25	7
V	—	30	40	—	20	40	30	30	50	0	15
Sc	7.8	5.9	7.4	9.9	4.5	7.6	5.6	7.2	10.2	3.9	2.2
Ni	20	10	13	15	10	10	10	10	20	10	5
Co	8.0	6.4	4.6	8.7	4.1	4.2	3.8	4.3	6.8	3.1	1.9
Ga	13	10	14	15	9	13	10	11	16	9	5
As	0.8	0.5	2.2	0.5	2.5	1.5	0.8	0.6	1.2	0.5	5.1
Zn	40	24	60	40	35	20	30	30	40	25	5
Sb	0.3	0.1	1.9	0.2	1.7	0.2	0.1	0.2	0.2	0.1	0.2
Au	0.01	0.04	0.02	0.01	0.08	0.02	0.04	0.06	0.04	0.02	0.02
Th	10.0	8.3	11.5	12.4	6.0	9.4	6.5	8.5	8.8	5.6	3.7
U	4.5	2.3	3.6	4.1	2.4	4.1	1.9	2.4	3.5	1.8	1.4
Zr	270	230	210	310	100	210	100	140	140	120	100
Hf	8.3	6.7	6.4	8.9	3.1	7.6	2.8	4.1	4.0	3.6	3.1
Ta	1.3	1.1	2.9	1.6	0.8	1.4	1.1	1.5	1.8	1.0	0.4
Y	37	31	24	36	19	27	16	16	15	16	14
La	31.8	22.1	29.2	32.9	24.6	23.0	18.8	18.3	24.3	16.6	12.3
Ce	70	54	61	72	53	48	40	41	44	37	28
Nd	31	24	27	35	22	22	20	19	21	16	12
Sm	7.40	4.70	4.74	5.70	3.86	4.32	3.60	3.62	3.46	3.00	2.47
Eu	1.15	0.90	0.72	1.15	0.68	0.70	0.53	0.56	0.64	0.48	0.45
Tb	0.86	0.80	0.68	1.00	0.55	0.82	0.48	0.48	0.48	0.36	0.37
Dy	—	6.0	4.9	—	3.6	5.5	4.4	3.4	3.5	—	2.3
Tm	0.6	0.4	0.4	0.6	0.2	—	0.2	0.3	0.3	0.3	0.2
Yb	4.50	3.01	2.67	4.06	1.82	3.14	1.56	1.85	1.81	1.66	1.37
Lu	0.69	0.48	0.40	0.67	0.28	0.50	0.25	0.30	0.29	0.26	0.21

and SiO_2 for argillites and, if the uncertainty is not large, limestones. The ratio TiO_2/Al_2O_3 appears to be constant over the range in metamorphic grade at a value of ~0.06; K_2O/Al_2O_3 appears to be constant also, but shows more scatter than TiO_2/Al_2O_3; SiO_2/Al_2O_3 shows considerable scatter with no obvious trend. The scatter indicates that there is a significant dependence of the chemistry on the protolith; if there is any systematic dependence on grade, it is well masked by premetamorphic chemical variability.

The variability in the chemistry of the argillites is examined using the statistical technique of analysis of variance (ANOVA). This technique determines the probability that two or more samples come from one population; this is the null hypothesis. The statistic used to test the hypothesis is the F value, which is calculated from the variances in the samples. The probability that an F value represents samples from one population depends on the number of independent variables, or degrees of freedom. In the present case, two hypotheses are tested. The first is that there is no difference between cycle 1 and cycle 2 argillites; the second is that there is no difference across metamorphic grade. There are seven variables in each test; these are the weight ratios of the oxides SiO_2, TiO_2, Fe_2O_3, MgO, CaO, Na_2O, and K_2O to Al_2O_3. The ANOVA can be applied individually to each ratio, but the hypotheses are designed to test the variances in all seven ratios simultaneously. The routines used to calculate the probabilities are the General Linear Models of the Statistical Analysis System (SAS, 1982). An excellent description of multivariate statistical methods is given by Morrison (1976).

The first hypothesis tests the equivalence of the stratigraphic cycles, which is a balanced design because there are 11 samples from each cycle. The results of the analysis are given in Table 3, and the 95% confidence inter-

TABLE 2B.   Whole-rock analyses for cycle 2 argillites

Sample:	16H-86	3H-40	3H-39	17H-87	20H-100	5H-44	23H-135	8H-59	7H-54A	11H-117	12H-123
SiO_2	49.50	51.10	54.00	57.50	51.50	46.80	60.50	51.00	58.80	60.60	51.50
TiO_2	0.30	0.30	0.84	0.70	0.40	0.60	0.70	0.60	1.00	0.30	0.40
Al_2O_3	5.60	5.10	12.67	11.80	6.40	11.60	12.70	12.80	17.40	5.30	5.20
Fe_2O_3	3.00	2.30	3.87	3.10	2.40	4.20	4.80	3.90	4.70	1.00	1.80
MnO	0.12	0.26	0.08	0.05	0.26	0.07	0.05	0.06	0.03	0.03	0.07
MgO	3.00	2.00	3.60	3.70	2.00	4.40	4.00	6.40	4.40	1.00	1.00
CaO	35.60	39.20	17.40	13.80	35.90	21.90	9.90	17.50	8.70	16.70	21.00
Na_2O	0.36	0.44	1.49	1.05	0.45	0.50	1.10	1.06	0.85	0.67	0.54
K_2O	1.05	0.23	4.70	7.20	0.22	2.84	4.20	3.10	4.60	1.80	1.80
P_2O_5	0.28	0.26	0.12	0.10	0.40	0.24	0.15	0.19	0.21	0.11	0.27
H_2O	0.24	0.39	0.52	0.22	0.09	0.25	0.69	0.28	0.35	0.45	0.45
CO_2	1.29	0.57	0.56	0.51	0.03	6.97	1.27	2.30	0.00	13.02	16.48
Total	100.34	102.15	99.85	99.73	100.05	100.37	100.06	99.19	101.04	100.98	100.51

Trace elements (ppm)

	16H-86	3H-40	3H-39	17H-87	20H-100	5H-44	23H-135	8H-59	7H-54A	11H-117	12H-123
S	97	49	87	11	76	10500	5800	—	12000	130	68
F	1100	330	1000	52	530	1030	364	—	4300	400	540
Cl	200	23	160	14	26	25	72	—	130	25	110
Cs	1.3	0.7	—	7.7	0.7	4.8	8.9	8.4	14.4	1.6	2.9
Rb	60	15	236	400	11	110	160	200	250	50	60
Ba	50	70	—	1300	50	310	590	430	520	320	290
Pb	15	5	20	66	6	8	7	9	6	22	8
Sr	670	460	974	1210	570	670	320	550	500	290	290
Cr	35	25	—	60	27	60	60	80	90	10	14
V	20	20	—	40	20	50	40	70	80	20	20
Sc	5.5	5.0	—	9.9	5.3	9.5	12.0	10.0	14.0	3.7	3.8
Ni	10	15	—	20	10	15	15	40	30	5	10
Co	6.3	7.0	—	7.5	5.7	6.9	8.6	9.4	14.0	1.7	3.1
Ga	11	9	16	13	10	15	17	17	19	7	8
As	2.20	0.36	—	0.80	0.70	0.76	1.00	0.69	1.20	4.50	9.10
Zn	80	30	—	70	30	70	40	50	50	20	20
Sb	1.80	0.06	—	0.80	0.30	0.28	0.32	0.36	0.60	0.70	0.45
Au	0.11	0.06	—	0.08	0.02	0.01	0.01	0.03	0.04	0.01	0.04
Th	7.1	6.2	14.0	13.1	6.1	11.4	13.0	11.9	16.0	6.5	6.7
U	3.3	1.6	—	5.6	1.7	4.0	4.9	2.6	6.3	2.5	2.0
Zr	150	100	—	240	150	150	240	110	180	200	240
Hf	4.4	2.9	—	7.5	4.8	4.1	9.1	3.4	5.9	6.1	7.2
Ta	0.74	0.57	—	1.60	0.70	1.20	1.70	0.91	1.70	0.61	0.72
Y	26	29	35	22	31	29	37	14	29	24	27
La	35.5	29.9	—	24.6	21.2	35.0	39.3	34.0	50.0	18.1	18.9
Ce	70	60	—	48	48	76	80	65	90	43	50
Nd	27	25	—	25	22	32	3.4	27	39	20	20
Sm	5.9	4.8	—	5.2	4.6	5.8	5.7	3.7	6.5	4.7	4.0
Eu	1.10	0.67	—	0.60	0.81	1.05	1.05	0.91	1.00	0.68	0.80
Tb	0.64	0.72	—	0.60	0.70	0.66	0.92	0.42	0.62	0.60	0.60
Dy	4.8	5.4	—	4.6	5.1	5.0	6.5	2.8	5.6	4.2	5.0
Tm	0.41	0.43	—	0.48	—	0.48	0.51	—	0.54	0.40	0.43
Yb	2.95	3.04	—	3.45	2.90	3.30	4.40	1.99	3.90	2.90	3.00
Lu	0.43	0.44	—	0.53	0.44	0.47	0.67	0.26	0.57	0.44	0.44

vals about the means of SiO_2/Al_2O_3 and K_2O/Al_2O_3 are shown in Figure 5. None of the means of the oxide ratios for the two cycles falls outside the 95% confidence interval, and the F test fails to reject the null hypothesis at the 5% level. This means that there is no statistically significant difference in chemistry between the two cycles.

The second hypothesis tests the equivalence in chemistry over the three metamorphic grades. The test applies to all three groups and not to two at a time. The numbers of samples in the three categories *unmetamorphosed, low grade,* and *high grade* are not equal. There are only 3 unmetamorphosed, 6 low-grade, and 13 high-grade samples. The analysis of variance is unbalanced, and the errors are standardized to the number of samples in each category. The results are shown in Table 4, and the 95% confidence limits on the means are shown for SiO_2/Al_2O_3 and K_2O/Al_2O_3 in Figure 6. Only the SiO_2/Al_2O_3 ratios show significant differences over the range in grade; all others

show no differences significant at the 5% level. The resulting F statistic indicates that the null hypothesis can be rejected, mainly because of the differences in the SiO_2/Al_2O_3 ratios. A possible conclusion is that SiO_2 was lost, relative to Al_2O_3, during metamorphism. If the infiltrating fluid was undersaturated in SiO_2, then metasomatic loss of SiO_2 to the fluid could explain the lower SiO_2/Al_2O_3 ratio in the unmetamorphosed rocks. Metasomatic loss of SiO_2 in excess of the buffering capacity of the rock must be represented by a change in the mineral assemblage resulting from systematic changes in the chemical potential of the diffusing or infiltrating component (Thompson, 1959; Korzhinskii, 1965), which is imposed on the system like T, P, and μ_{H_2O}. The capacity of the rock to buffer the SiO_2 activity in the fluid certainly was not exceeded. The μ_{SiO_2} remained constant across the diopside isograd, which separates the unmetamorphosed from the low-grade rocks, because quartz occurs in sam-

TABLE 2C. Whole-rock analyses for 10H traverse

Sample:	10H-102	10H-103	10H-104	10H-105	10H-106	10H-108	10H-107
SiO_2	44.24	42.72	45.83	37.64	48.23	33.40	4.80
TiO_2	0.67	0.52	0.45	0.53	0.38	0.34	0.04
Al_2O_3	11.40	9.84	8.71	7.53	3.93	2.96	0.34
Fe_2O_3	8.03	4.28	3.61	2.03	1.52	2.38	1.00
MnO	0.43	0.32	0.32	0.04	0.06	0.05	0.04
MgO	2.90	4.00	3.40	2.10	1.40	3.00	3.40
CaO	27.04	34.70	34.25	34.15	38.84	41.20	49.40
Na_2O	1.14	0.07	0.40	0.76	0.28	0.18	0.04
K_2O	0.21	0.02	0.09	2.26	1.78	1.18	0.07
P_2O_5	0.11	0.09	0.09	0.19	0.28	0.23	0.11
H_2O	0.65	0.56	0.86	0.18	0.14	0.09	—
CO_2	3.17	3.74	2.74	13.20	2.88	15.95	40.20
Total	99.99	100.86	100.75	100.61	99.72	100.96	99.44

Trace elements (ppm)

	10H-102	10H-103	10H-104	10H-105	10H-106	10H-108	10H-107
S	24	66	104	800	20	170	—
F	1100	2700	3200	400	630	790	—
Cl	25	36	250	310	28	25	—
Cs	1.1	0.29	0.44	2.4	2.7	2.4	0.15
Rb	16	1	4	108	108	78	4.3
Ba	110	40	50	330	530	160	25
Pb	4	9	7	15	22	32	—
Sr	700	267	320	768	710	712	940
Cr	100	70	65	55	25	20	2.8
V	50	50	50	40	20	20	<10
Sc	12.1	8.7	8.7	7.7	4.3	4.4	1.1
Ni	15	20	20	15	5	10	<10
Co	12	8.2	8	5.3	2.9	4.4	0.57
Ga	—	—	—	—	—	—	3
As	1.9	11.2	20	1	1.8	0.9	0.6
Zn	150	140	150	30	80	30	6
Sb	1.2	9.1	7.7	0.5	1.3	1.1	0.055
Au	0.02	0.025	0.035	0.007	0.01	0.01	0.01
Th	11.6	7.8	8.4	10	15.6	7.4	1.25
U	4.8	3.5	6	3.9	3.8	3.7	0.8
Zr	160	100	130	270	410	300	24
Hf	4.9	2.7	2.6	7.8	12	8	0.56
Ta	1.1	0.9	1.1	1.2	2	0.6	0.055
Y	32	21	17	25	37	24	7
La	35.6	27.4	25.6	22.5	19.9	16.1	4.6
Ce	67	48	48	51	60	47	12
Nd	35	25	21	22	24	20	5.6
Sm	5.37	3.85	3.98	4.67	5.69	4.48	1.15
Eu	0.96	0.77	0.61	0.74	0.69	0.72	0.2
Tb	0.9	0.6	0.51	0.7	1	0.68	0.16
Dy	6.3	4.2	3.4	5	7.6	4.6	—
Tm	0.43	0.34	0.29	0.41	0.63	0.36	—
Yb	3.4	2.22	1.84	2.74	4.44	2.6	0.56
Lu	0.54	0.35	0.34	0.45	0.71	0.45	0.092

ples from both groups. If the difference in the SiO_2/Al_2O_3 ratio resulted from dissolution, the minimum amount of infiltrating H_2O can be estimated from the solubility of silica, summarized by Walther and Helgeson (1977). The apparent loss from Table 4 is 5.9 kg SiO_2 per 1 kg Al_2O_3. The solubility of silica in H_2O at 2 kbar and 400 °C, approximate conditions at the diopside isograd, is about $0.032m$ (Walther and Helgeson, 1977). The amount of H_2O required to dissolve the apparent SiO_2 loss is about 3105 kg H_2O per 1 kg Al_2O_3. The amount of Al_2O_3 in the unmetamorphosed rocks ranges from 2 to 5%, implying fluid : rock ratios in excess of 60 by mass would have been required to cause the apparent loss of SiO_2. This ratio exceeds the fluid : rock ratio calculated from decarbonation, determined by Labotka et al. (1988), by a factor of more than 120. The large disparity in the fluid : rock ratio indicates that metasomatic dissolution of silica is not the major source of variability between the unmeta-

morphosed and low-grade rocks. In addition, the SiO_2/Al_2O_3 ratios shown in Figure 6 are higher in high-grade than in low-grade samples, although there is some overlap in the confidence intervals for the means. The change in the SiO_2/Al_2O_3 ratio is not systematic with grade, and the significantly different value for unmetamorphosed samples must result from the natural variability of the ratio in the protolith and from the very low number of samples in the unmetamorphosed group. The analysis of variance indicates that there is no detectable variability in the major-element chemistry, excepting CO_2, that results from stratigraphic position or metamorphic grade.

The major-element variance must have been inherited from the protolith. The range in bulk-rock composition is shown in Figure 7, which is a plot of CaO, SiO_2, and Al_2O_3 for argillites and marbles. The rocks contain both carbonate and siliciclastic components. Calcite is clearly the major carbonate component, but the scatter in the

TABLE 2D. Whole-rock analyses for cycle 2 limestones

Sample:	14H-81	16H-85	3H-38A	18H-90	20H-99
SiO_2	2.70	1.60	1.40	1.70	1.10
TiO_2	0.02	0.01	0.01	0.02	0.01
Al_2O_3	0.29	0.17	0.17	0.13	0.13
Fe_2O_3	0.35	0.28	0.28	0.25	0.29
MnO	0.02	0.01	0.01	0.02	0.01
MgO	6.00	3.10	5.00	3.00	3.40
CaO	49.10	51.40	50.60	52.00	51.20
Na_2O	0.04	0.03	0.03	0.01	0.04
K_2O	0.04	0.02	0.02	0.01	0.01
P_2O_5	0.06	0.06	0.05	0.04	0.05
CO_2	41.50	43.10	43.30	42.70	42.90
Total	100.11	99.78	100.87	99.88	99.14
Trace elements (ppm)					
Cs	0.190	0.220	0.055	0.130	0.026
Rb	1.9	1.5	1.3	0.6	0.3
Ba	30	30	30	20	20
Pb	5	1	1	1	4
Sr	770	900	880	800	840
Cr	2.60	1.40	1.40	1.30	1.20
V	—	<10	<10	<10	<10
Sc	0.25	0.14	0.13	0.08	0.15
Ni	<5	<5	<5	<10	<10
Co	0.190	0.110	0.094	0.090	0.130
Ga	3	3	3	2	3
As	1.00	0.55	0.20	0.65	0.90
Zn	4	4	2	4	4
Sb	0.02	0.13	0.04	0.09	0.01
Au	0.090	0.060	0.040	0.030	0.010
Th	0.40	0.14	0.13	0.09	0.13
U	0.85	0.60	0.50	0.30	0.40
Zr	14	<10	<10	<10	<10
Hf	0.140	0.046	0.040	0.022	0.039
Ta	0.064	0.015	0.017	0.010	0.016
Y	0.6	0.7	0.8	—	1.0
La	1.30	0.85	0.67	0.62	0.91
Ce	3.0	1.5	1.3	1.2	1.2
Nd	2.0	1.0	1.5	2.0	2.0
Sm	0.35	0.29	0.18	0.15	0.20
Eu	0.036	0.020	0.020	0.015	0.016
Tb	0.024	0.011	0.010	0.010	0.010
Yb	0.079	0.051	0.040	0.027	0.045
Lu	0.021	0.001	0.010	0.006	0.006

SiO_2/Al_2O_3 ratio indicates there is not a single detrital component. The scatter could result from two or more source areas with different chemistries or for a differentiation process that occurred during transport or diagenesis of the detritus. Principal-components analysis was used to help determine the cause of the scatter. The weight percents of the oxides constitute a closed data set, which has a significant effect on principal components (Chayes and Trochimczk, 1978). Ca occurs almost exclusively in calcite and was, therefore, left out of the analysis to help alleviate the closure effect. Two of the seven principal components extracted from the covariances of the remaining oxides are shown in Table 5. These two account for 98% of the total variance in the major-element chemistry, other than calcite. The first, accounting for 89%, is dominated by SiO_2 with a minor contribution by Al_2O_3. The second, accounting for 9%, represents Al_2O_3, in a combination with K_2O, MgO, and minor FeO. The first component appears to represent quartz and, perhaps, feldspar, whereas the second appears to represent micas or clay minerals, which are rich in Al, K, Mg, and Fe. The principal-components analysis has separated the de-

trital component of the argillites by grain shape—rounded quartz and feldspar from platy micas. These two types of grains were probably mixed independently because of differences in transport characteristics during sedimentation. The scatter in the major-element chemistry is well explained as a mixture of three sedimentary components: calcite, quartzofeldspathic grains, and micas. The only clear metamorphic effect on the major-element chemistry is partial to nearly complete decarbonation of the low-grade and high-grade rocks.

TRACE-ELEMENT CHEMISTRY

Although there is no clear evidence for major-element metasomatism, trace elements could have migrated during the infiltration of the large volume of H_2O through the argillite layers. Trace elements rarely form separate phases in the argillites, and migration could have occurred if the concentrations in the rock and infiltrating fluid are out of equilibrium. The rock acts, in effect, like an ion-exchange column. The concentrations of several trace elements from the argillite samples are examined to determine whether the variances in the chemistry can be

TABLE 2D—*Continued*

5H-46	23H-136	8H-130	7H-55	11H-116	12H-122
1.30	1.90	2.60	1.20	1.60	1.10
0.02	0.01	0.03	0.01	0.01	0.02
0.20	0.20	0.67	0.18	0.23	0.12
0.21	0.21	0.24	0.14	0.19	0.17
0.01	0.03	0.01	0.01	0.02	0.01
3.20	2.00	1.00	1.90	2.20	2.50
51.30	52.80	52.50	52.80	52.60	52.30
0.02	0.03	0.11	0.02	0.01	0.04
0.04	0.02	0.06	0.03	0.03	0.02
0.05	0.05	0.09	0.06	0.05	0.04
42.40	43.60	43.00	45.00	43.70	45.20
98.75	100.85	100.31	101.35	100.63	101.52
		Trace elements (ppm)			
0.058	0.040	0.160	0.074	0.030	0.020
2.5	0.8	3.5	3.0	2.7	1.0
20	10	15	15	10	20
3	1	6	4	7	3
790	700	680	870	660	680
1.40	0.90	1.90	1.70	0.96	0.82
<10	<10	<10	<10	<10	<10
0.14	0.15	0.48	0.15	0.17	0.10
<5	<10	<5	<5	<5	<5
0.110	0.160	0.500	0.170	0.150	0.086
4	3	4	3	3	3
1.70	0.50	0.90	1.40	1.10	0.70
2	2	3	2	10	2
0.02	0.02	0.04	0.06	0.03	0.02
0.010	0.005	0.040	0.010	0.005	0.050
0.25	0.22	0.38	0.20	0.19	0.13
0.60	0.22	0.30	0.40	0.40	0.40
<10	<10	<10	<10	<10	<10
0.090	0.053	0.150	0.063	0.050	0.039
0.062	0.025	0.054	0.030	0.020	0.020
—	1.0	3.0	1.0	1.0	—
1.10	1.30	4.10	1.10	1.10	0.80
2.2	2.6	7.6	2.3	2.3	1.9
2.0	2.0	4.0	2.0	2.0	2.0
0.25	0.27	0.65	0.22	0.30	0.29
0.024	0.036	0.130	0.030	0.037	0.019
0.014	0.030	0.070	0.020	0.024	0.012
0.066	0.093	0.230	0.054	0.110	0.039
0.016	0.012	0.033	0.010	0.019	0.006
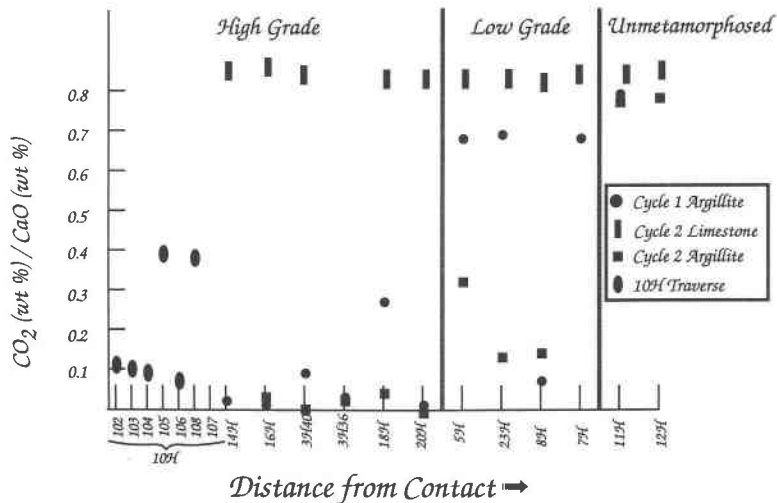
Fig. 2. Weight ratios of CO_2/CaO for argillite and limestone samples plotted with increasing distance from the contact with the stock. Solid symbols represent argillite samples; open symbols are limestones. The samples are described in Table 1, and their locations are shown in Fig. 1.
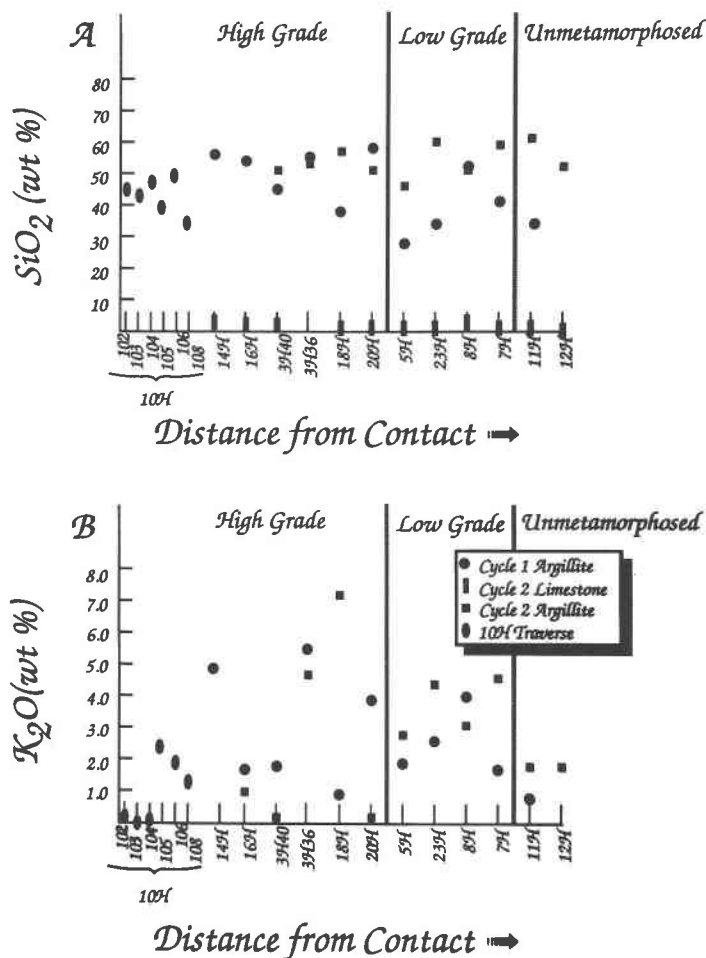
Fig. 3.   Absolute abundances of K₂O and SiO₂ in argillite samples as a function of distance from the contact. The scatter in the data results from both original variability in the protolith and loss of CO₂.

TABLE 3.   Analysis of variance of wt% oxide/wt% Al₂O₃ in argillite samples: Effects of stratigraphic cycle

Oxide	Cycle	n	Mean	Standard error	Minimum value	Maximum value	F value (2 DF)	Probability >F
SiO₂	1	11	5.968	0.545	3.958	9.773	0.47	0.502
	2	11	6.685	0.898	3.379	11.430		
TiO₂	1	11	0.064	0.002	0.050	0.074	2.36	0.140
	2	11	0.059	0.002	0.047	0.077		
Fe₂O₃	1	11	0.336	0.021	0.261	0.500	0.04	0.836
	2	11	0.344	0.029	0.189	0.536		
MgO	1	11	0.408	0.037	0.217	0.618	2.25	0.149
	2	11	0.333	0.034	0.189	0.536		
CaO	1	11	4.975	0.456	1.309	18.682	1.25	0.276
	2	11	3.083	0.227	0.500	7.686		
Na₂O	1	11	0.100	0.018	0.046	0.217	0.76	0.395
	2	11	0.084	0.008	0.043	0.126		
K₂O	1	11	0.314	0.036	0.170	0.516	0.45	0.509
	2	11	0.274	0.048	0.034	0.610		

Note: Test criterion for the hypothesis that the two stratigraphic cycles are equivalent: $F = 2.38$. The null hypothesis cannot be rejected at the 95% confidence limit.
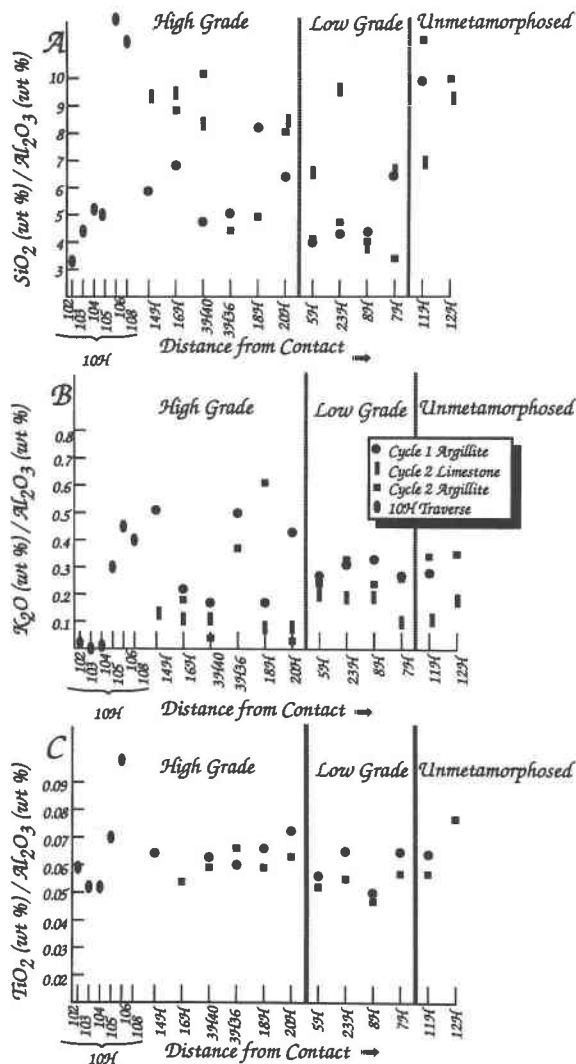
Fig. 4. Weight ratios of cations to Al_2O_3 vs. distance. The ratios eliminate the concentration effect that occurs during devolatilization. The variances in these data are analyzed to determine whether there are significant differences in chemistry with stratigraphic horizon or with metamorphic grade. The results are plotted in Figs. 5 and 6 and given in Tables 3 and 4. The limestone data are not shown in C because of the large uncertainty in the ratio TiO_2/Al_2O_3 in the limestones.

Fig. 5. Confidence intervals about the means for the ratios SiO_2/Al_2O_3 and K_2O/Al_2O_3 testing the hypothesis of no chemical difference between cycle 1 and cycle 2 argillites. The null hypothesis cannot be rejected at the 5% significance level (Table 3).

explained by simple devolatilization, in accordance with the results from the variances in the major-element chemistry, or whether there are systematic deviations that can be ascribed to exchange with the infiltrating fluid. The concentrations of 34 trace elements are given in Table 2; subsets of these 34 are described individually to keep the amount of information manageable. These subsets include the alkali and alkaline-earth elements, transition-metal elements, rare-earth elements, and other large-ion lithophile elements. Much of the discussion centers on the multiple correlations among the major and trace elements with similar geochemical behaviors; Table 6 shows the correlation coefficients for 25 selected representatives of major and trace elements from these groups.

The concentrations of most trace elements increase with increasing metamorphic grade, as expected from loss of CO_2. For example, Figure 8 shows the 95% confidence intervals about the means of Rb, Sr, Cr, and La. These elements are chosen to represent the geochemical groupings listed above. In nearly all cases the confidence intervals for the three grades of metamorphism overlap, but the means are generally higher for the low-grade and high-grade rocks than for the unmetamorphosed rocks. This increase in concentration can simply result from the devolatilization, which causes a concentration of the nonvolatile residua.

If ion exchange with an infiltrating fluid has not occurred, the concentration ratio of the trace elements to geochemically similar trace- and major-elements should be constant over the range in grade. The constancy of the ratios will be manifested in high correlation coefficients among the geochemically similar elements. Table 6 shows that the six correlation coefficients among Rb, Ba, Cs, and K are all greater than 0.70, and half are greater than 0.90. All these have nearly constant interelement ratios; whither goes K, so go Ba, Cs, and Rb. If the abundance of K has not been altered by the infiltrating fluid, then neither have the abundances of the other alkalis and Ba.

The correlation between the abundances of Ca and Sr, both alkaline earths, is not very high; the correlation coefficient is 0.42. In fact, Sr is not highly correlated with any element. Figure 9 shows a plot of CaO vs. Sr and the 95% confidence interval for the ratio Sr/CaO for unmetamorphosed, low-grade, and high-grade rocks. With the exception of three samples, Sr concentration is nearly constant at about 500 ppm. The three samples have considerably more Sr, up to 1200 ppm, with only about 15% CaO. The factor means for Sr/CaO at the three levels of metamorphism (Fig. 9), are not different from one another at the 95% confidence level, although the means for the meta-

TABLE 4. Analysis of variance of wt% oxide/wt% Al_2O_3 in argillite samples: Effects of metamorphic grade

Oxide	Grade*	n	Mean	Standard error	Minimum value	Maximum value	F value (2 DF)	Probability >F
SiO_2	U	3	10.370	0.533	9.773	11.430	12.36	0.0004
	L	6	4.451	0.429	3.379	6.397		
	H	13	6.259	0.547	3.984	10.020		
TiO_2	U	3	0.066	0.006	0.057	0.077	1.03	0.376
	L	6	0.058	0.002	0.052	0.065		
	H	13	0.061	0.002	0.047	0.074		
Fe_2O_3	U	3	0.287	0.049	0.189	0.346	1.63	0.221
	L	6	0.313	0.019	0.270	0.378		
	H	13	0.364	0.025	0.261	0.536		
MgO	U	3	0.309	0.118	0.189	0.545	0.44	0.650
	L	6	0.384	0.040	0.253	0.508		
	H	13	0.379	0.032	0.217	0.618		
CaO	U	3	8.624	2.904	3.151	18.682	2.87	0.082
	L	6	2.634	0.303	0.500	4.681		
	H	13	3.613	0.209	1.169	9.065		
Na_2O	U	3	0.122	0.009	0.104	0.136	2.98	0.075
	L	6	0.059	0.007	0.245	0.331		
	H	13	0.100	0.014	0.046	0.217		
K_2O	U	3	0.323	0.020	0.282	0.346	0.09	0.918
	L	6	0.280	0.013	0.245	0.331		
	H	13	0.294	0.050	0.034	0.610		

Note: Test criterion for the hypothesis that effects of metamorphic grade are equivalent: $F = 3.10$. The null hypothesis can be rejected at the 95% confidence limit.
* U = unmetamorphosed, L = low grade, H = high grade.

morphosed samples are greater than the mean for the unmetamorphosed samples. The three samples with high concentrations of Sr could have been enriched in Sr relative to Ca, but, if so, the enrichment was selective rather than systematic with grade. The three samples with high Sr (17H-87, 3H-39, and 3H-36, Table 2) are also enriched in Ba (1300 ppm in 17H-87), Rb, and K. The high values of these elements indicate that rocks were either originally enriched in feldspars and micas, or the sample was enriched in the feldspar components during recrystallization. The high-grade samples are very coarse grained because of the abundance of garnet and vesuvianite. It it possible that during the formation of these large minerals, the feldspars became abnormally concentrated, indicating migration during crystal growth over distances on the order of the 5-kg sample size (~2 L). The high alkali values, then, could be attributed to the heterogeneous distribution of feldspar during recrystallization.

Cr is highly correlated to other highly charged cations and to Fe. These include Al, Ti, Sc, U, Th, and La. Similarly, all the rare-earth elements are highly correlated with one another and with Si and Al. The high degree of correlation among all these trace elements indicates that their abundances were not altered during metamorphism, except for the concentration effect caused by devolatilization. The rare-earth patterns themselves, shown in Figure 10, are light-rare-earth enriched, have a slight negative Eu anomaly, and are typical of granitic rocks, the probable source of the clastic components of the Big Horse Limestone. The pattern is similar to those of the granitic
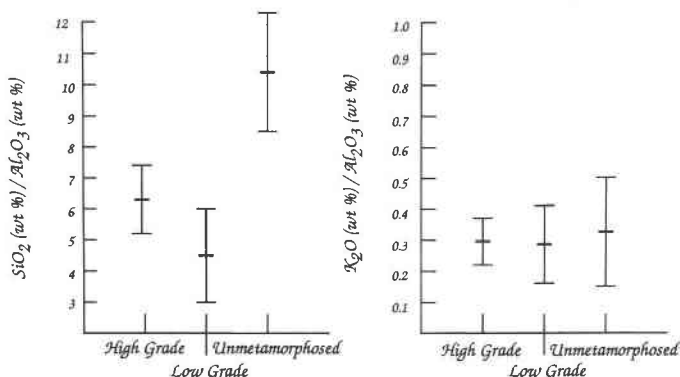
95% Confidence Intervals for Means

Fig. 6. Confidence intervals about the means for the ratios SiO_2/Al_2O_3 and K_2O/Al_2O_3 testing the hypothesis of no chemical difference in argillite samples over metamorphic grade. The hypothesis can be rejected at the 5% level of significance because of the high ratio of SiO_2/Al_2O_3 in the unmetamorphosed samples.

TABLE 5. Principal-components analysis of argillites

			Correlation coefficients				
	SiO_2	TiO_2	Al_2O_3	Fe_2O_3	MgO	Na_2O	K_2O
SiO_2	1.00						
TiO_2	0.57	1.00					
Al_2O_3	0.54	0.95	1.00				
Fe_2O_3	0.55	0.80	0.86	1.00			
MgO	0.19	0.54	0.73	0.66	1.00		
Na_2O	0.58	0.62	0.49	0.36	0.16	1.00	
K_2O	0.48	0.76	0.74	0.53	0.47	0.64	1.00

	Principal components	
	Number 1	Number 2
SiO_2	0.97	−0.23
TiO_2	0.01	0.04
Al_2O_3	0.20	0.83
Fe_2O_3	0.05	0.18
MgO	0.04	0.36
Na_2O	0.02	0.02
K_2O	0.09	0.30
% of total variance	88.9	9.2

stock (Nabelek et al., 1986), but the bulk of the stock does not contain Eu anomalies as prominent as those of the Big Horse Limestone Member. The patterns of the limestone are similar to the parent of the melts that gave rise to the Notch Peak stock, as proposed by Nabelek et al. (1986).

Finally, the correlations among all the variables are examined using the technique of cluster analysis. This method groups variables having the highest correlations and successively subdivides the groups into smaller, closely related sets of variables. There are many methods of determining the relations among the variables, and each method gives slightly different results. The cluster-analysis technique, thus, does not have a rigorous statistical basis. The results cannot be assigned a degree of significance. However, the clustering will give an indication of similarly behaved elements. If the analysis singles out one or two elements that seem to be unrelated to all others, these might be considered to have had their abundances modulated by processes other than mixing of components in the sedimentary protolith. In the present case, Sr abundance possibly has been altered during metamorphism because of its poor correlation with other elements, as indicated by Figure 9. If so, the cluster analysis should show the dissimilarity between Sr and the other variables. The method used is the centroid method in which similarity is measured as similar distances from the center of the data; the procedures is SAS (1982) VARCLUS. The resulting tree diagram, which shows the similarities among variables (the clusters), is shown in Figure 11. The elements form few clusters, and the majority of elements that occur in the silicate components are all clustered together. In particular, K, Rb, Ba, and Sr—those that occur in alkali feldspar—are all clustered. Ca is clustered only with a few elements, as expected, because Ca is primarily associated with the carbonate component of the argillite. Figure 11 also shows a tree that results from clustering the variables from both the argillites and the limestones. The tree is similar to that
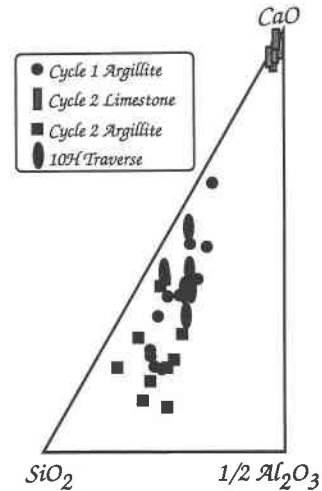

Fig. 7. Weight ratios of SiO_2, Al_2O_3, and CaO for all samples showing that calcite is a major component in the protolith and that more than one siliciclastic component contributed to the noncarbonate fraction of the protolith.
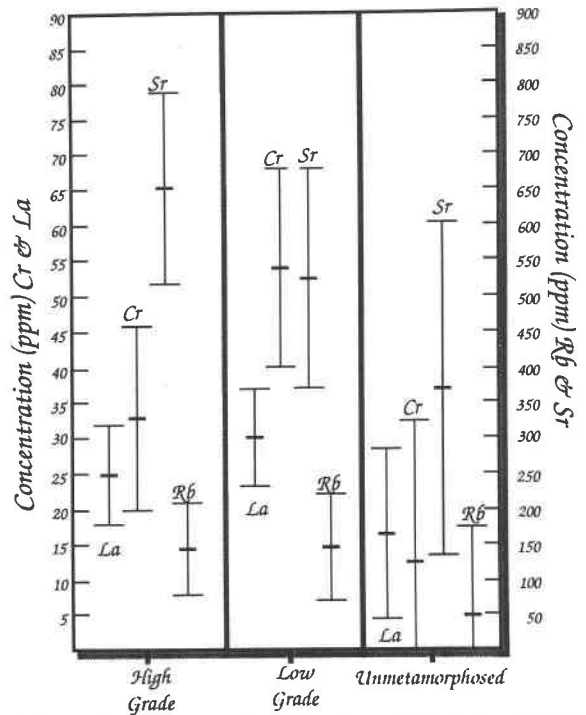

Fig. 8. The means of the four elements La, Cr, Sr, and Rb in argillites at different metamorphic grades are used to illustrate the behavior of REE and large-ion lithophile elements, transition metals, alkaline earths, and alkalis, respectively, during devolatilization. Trace elements tend to be concentrated at high grade, but the confidence intervals about the means overlap for any one element at different metamorphic grades. There is no significant systematic difference in elemental abundances over the range in metamorphic grade. The scales for Cr and La are on the left, and those for Rb and Sr are on the right.

TABLE 6.   Correlation coefficients for 25 major, minor, and trace elements in argillites

	Si	Al	Fe	Mg	Mn	Ti	Ca	Na	K	P	Cs	Rb
Si	1.00											
Al	**0.77**	1.00										
Fe	0.63	**0.84**	1.00									
Mg	0.01	0.32	0.24	1.00								
Mn	0.28	0.28	0.50	0.05	1.00							
Ti	**0.83**	**0.96**	**0.80**	0.26	0.25	1.00						
Ca	**−0.96**	**−0.90**	**−0.73**	−0.11	−0.29	**−0.92**	1.00					
Na	0.67	0.67	0.54	−0.13	0.32	**0.73**	**−0.73**	1.00				
K	0.61	**0.70**	0.38	0.03	0.04	**0.73**	**−0.73**	**0.71**	1.00			
P	0.39	0.15	0.14	−0.22	0.40	0.25	−0.33	0.34	0.29	1.00		
Cs	0.54	**0.77**	0.47	0.36	−0.03	**0.75**	−0.68	0.57	**0.82**	0.12	1.00	
Rb	0.56	0.69	0.38	0.09	0.06	0.69	−0.68	0.68	**0.96**	0.25	**0.83**	1.00
Ba	0.56	0.61	0.33	−0.01	0.12	0.64	−0.65	0.63	**0.94**	0.21	**0.73**	**0.94**
Sr	−0.50	−0.33	−0.25	−0.17	−0.11	−0.34	0.42	−0.22	0.07	−0.10	−0.06	0.20
Cr	0.61	**0.90**	**0.91**	0.40	0.36	**0.84**	**−0.74**	0.54	0.46	0.00	0.61	0.51
Sc	**0.75**	**0.97**	**0.89**	0.32	0.37	**0.94**	**−0.87**	0.67	0.66	0.14	**0.75**	0.66
As	0.17	0.08	0.14	0.19	0.30	0.04	−0.11	−0.14	−0.24	−0.14	−0.21	−0.25
Sb	0.16	0.19	0.30	0.46	0.36	0.13	−0.13	−0.19	−0.23	−0.22	−0.18	−0.19
Th	**0.73**	**0.75**	0.62	0.19	0.30	**0.81**	**−0.77**	0.55	0.59	0.30	0.56	0.63
U	**0.72**	**0.81**	**0.76**	0.25	0.31	**0.84**	**−0.80**	0.58	0.63	0.11	0.64	0.65
Hf	**0.78**	0.53	0.44	−0.13	0.20	0.69	**−0.74**	0.64	0.65	0.45	0.48	0.61
Ta	0.69	**0.77**	0.58	0.08	0.15	**0.82**	**−0.76**	0.54	0.65	0.17	0.58	0.61
La	**0.82**	**0.89**	**0.84**	0.28	0.37	**0.87**	**−0.88**	0.59	0.56	0.31	0.67	0.56
Sm	**0.90**	**0.76**	**0.72**	0.06	0.34	**0.83**	**−0.89**	0.61	0.61	0.47	0.53	0.58
Lu	**0.87**	0.69	0.66	0.01	0.39	**0.79**	**−0.85**	0.67	0.63	0.47	0.52	0.60
	Si	Al	Fe	Mg	Mn	Ti	Ca	Na	K	P	Cs	Rb

Note: Correlation coefficients with absolute values greater than or equal to 0.7 are shown in boldface.
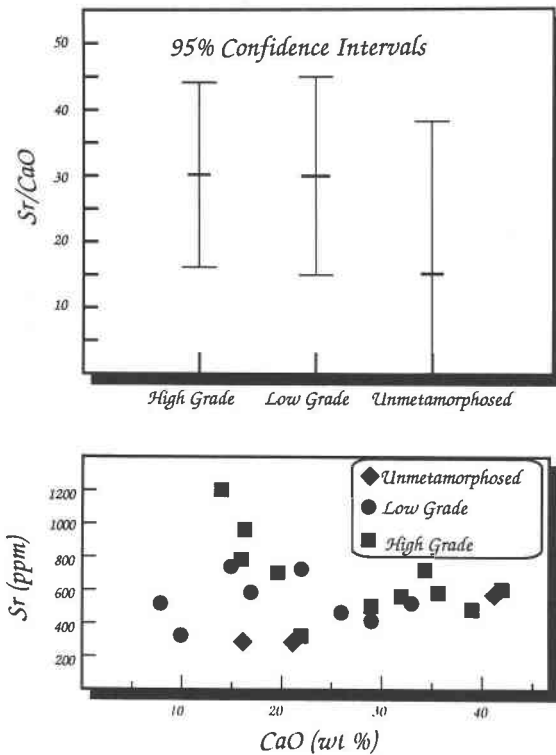

Fig. 9.   Sr shows a significant scatter in abundance, particularly for high-grade samples. The Sr/CaO plot shows there is no significant difference over the range in metamorphic grade, but there is a poor correlation between Sr and CaO, as illustrated in the lower plot. The samples that contain >800 ppm Sr also contain high abundances of Ba, Rb, and K, indicating that Sr occurs in feldspar as well as the carbonate component. The low

for the argillite data only, except that now Ca and Sr are grouped in a cluster that is completely separate from all other elements. This clustering results from the dominance of calcite as a component in both rock types. There is no indication of variability in the abundance of any element that can be the result of metasomatic processes.

SUMMARY AND CONCLUSIONS

The variability in the concentrations of major and trace elements in the limestones and argillites of the Big Horse Limestone Member can be reliably ascribed to original variability in the amounts of the sedimentary components composing the protolith. The range in major-element composition is accurately described as a three-component mixture of calcite, quartz (and, perhaps, feldspar), and mica or clay minerals. The last two, terrigenous components were probably sorted independently in the sedimentary environment because of the difference in shape between equant quartz and feldspar grains and platy mica grains. In the argillites, the absolute abundances of major elements tended to increase with metamorphic grade, but the increase is simply related to the concentration effect that occurred during loss of CO_2 with metamorphism. The ratios of elements remained constant, with the possible exception of SiO_2/Al_2O_3. Considering even the vari-

correlation coefficient between Sr and Ca must result from this duality. The high concentration of Sr in some high-grade samples indicates that feldspar components must have been abnormally concentrated during recrystallization of coarse-grained vesuvianite + garnet rocks.

TABLE 6—*Continued*

Ba	Sr	Cr	Sc	As	Sb	Th	U	Hf	Ta	La	Sm	Lu
1.00												
0.21	1.00											
0.43	−0.19	1.00										
0.60	−0.26	**0.94**	1.00									
−0.19	−0.48	019	0.11	1.00								
−0.16	−0.36	0.37	0.25	**0.83**	1.00							
0.61	−0.09	**0.71**	**0.75**	0.06	0.18	1.00						
0.62	−0.17	**0.83**	**0.88**	0.28	0.37	**0.77**	1.00					
0.68	−0.18	0.41	0.57	−0.05	−0.03	0.69	0.68	1.00				
0.65	−0.21	0.61	**0.75**	0.00	0.14	**0.76**	**0.74**	**0.72**	1.00			
0.48	−0.36	**0.85**	**0.91**	0.09	0.22	**0.74**	**0.82**	0.60	**0.70**	1.00		
0.56	−0.30	0.68	**0.79**	0.05	0.14	**0.80**	**0.82**	**0.82**	**0.72**	**0.90**	1.00	
0.63	−0.27	0.61	**0.74**	0.03	0.11	**0.75**	**0.80**	**0.92**	**0.72**	**0.81**	**0.96**	1.00
Ba	Sr	Cr	Sc	As	Sb	Th	U	Hf	Ta	La	Sm	Lu

ations in SiO_2/Al_2O_3, there are no systematic differences in major-element ratios with metamorphic grade. At the 95% confidence level, the major-element composition of the argillites is constant, except for loss of CO_2.

The abundances of the trace elements in the argillites are closely tied to those of the geochemically similar major elements. Alkalis and alkaline earths are strongly correlated with K, the rare earths are strongly correlated with each other and with Si and Al, transition metals are strongly correlated with Al, Fe, and Ti, and all elements except Sr are negatively correlated with Ca. The trace elements are strongly connected to the noncarbonate components. The only exception is Sr. Sr is only weakly correlated with Ca and poorly correlated with Rb and Ba. A cluster analysis of major and trace elements in the argillites shows that Sr behaves most similarly to Rb, Ba, and K. A cluster analysis that includes the limestone sam-
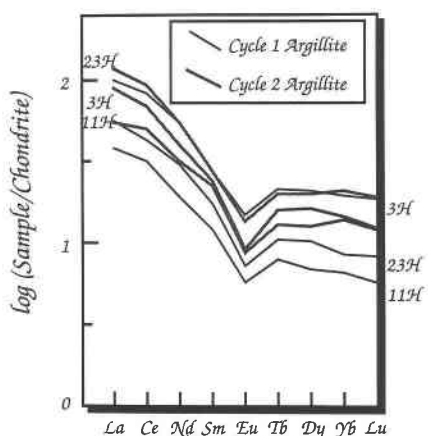

Fig. 10. Chondrite-normalized abundances of some rare-earth elements in representative argillite samples. The abscissa is compressed, as it does not include several REE that were not analyzed. The effect of this compression is a steeper slope than conventionally seen. There is no significant difference in the shapes of the patterns with respect to either grade or stratigraphic cycle. 3H is a high-grade locality, 23H is a low-grade locality, and samples from 11H are unmetamorphosed.
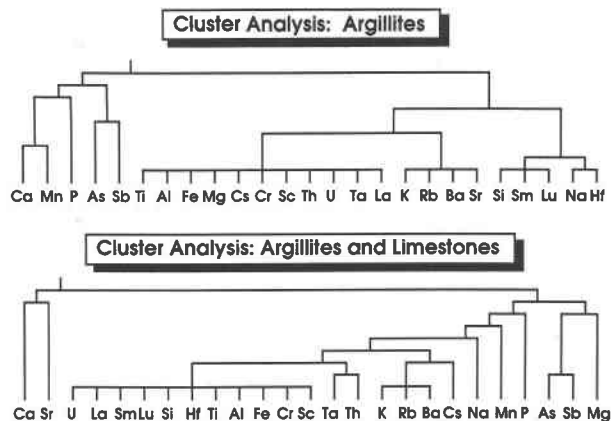

Fig. 11. Cluster analyses on the correlation coefficients of 25 major, minor, and trace elements. The top tree shows the familiality of elements from the argillites. Elements that occur in silicate minerals form one branch; whereas, elements generally occurring in carbonate, phosphate, and sulfide minerals form a second. In this tree, Sr is grouped with the elements found principally in K-feldspar. The lower tree includes limestone samples. In this tree, the affinity of Sr for calcite is clearly demonstrated. No element is singled out; there is no evidence for systematic differences in variance with metamorphic grade. There is no evidence for migration of any element during metamorphism.

ples groups Sr and Ca and separates them from all other elements. The weak correlations between Sr and Ca, Rb, and Ba in the argillites probably resulted from the tendency for Sr to occur both in alkali feldspars and in carbonate minerals. The poor correlations stemmed from the independent nature of these two mineral components in the protolith. The samples that are extremely enriched in Sr, Ba, and Rb contain an abnormally high concentration of feldspar, indicating that feldspar components locally migrated over volumes of about 2 L during metamorphism.

The petrologic study of Hover-Granath et al. (1983) and the stable-isotope study of Nabelek et al. (1984) have shown that substantial amounts of externally derived H_2O interacted with the argillites of the Big Horse Limestone Member. The reactions that occurred during metamorphism resulted in the loss of as much as 30 wt% CO_2. Labotka et al. (1985) estimated that this loss resulted in a volume reduction of the solid rock by as much as a factor of ⅓. Despite the nearly complete loss of CO_2 that occurred during metamorphism of the argillites, the bulk composition of all other elements remained within the limits of the variability of the protolith. The only change in chemistry during metamorphism of the Big Horse Limestone Member that can be demonstrated is loss of CO_2.

REFERENCES CITED

Chayes, F., and Trochimczk, J. (1978) An effect of closure of the structure of principal components. Mathematical Geology, 10, 323–333.

Feldman, M.D., and Papike, J.J. (1981) Metamorphic fluid composition from the Notch Peak aureole, Utah (abs.). EOS, 62, 435.

Ferry, J.M. (1982) A comparative geochemical study of pelitic schists and metamorphosed carbonate rocks from south-central Maine, USA. Contributions to Mineralogy and Petrology, 80, 59–72.

Hintze, L.F. (1974) Preliminary geologic map of the Notch Peak quadrangle Millard County, Utah. U.S. Geological Survey Miscellaneous Field Studies Map MF-636.

Hover-Granath, V.C., Papike, J.J., and Labotka, T.C. (1983) The Notch Peak contact metamorphic aureole, Utah: Petrology of the Big Horse Limestone Member of the Orr Formation. Geological Society of America Bulletin, 94, 889–906.

Korzhinskii, D.S. (1965) The theory of systems with perfectly mobile components and processes of mineral formation. American Journal of Science, 263, 193–205.

Kretz, Ralph. (1983) Symbols for rock-forming minerals. American Mineralogist, 68, 277–279.

Labotka, T.C., White, C.E., and Papike, J.J. (1984) The evolution of water in the contact-metamorphic aureole of the Duluth Complex, Minnesota. Geological Society of America Bulletin, 95, 788–804.

Labotka, T.C., Papike, J.J., and Nabelek, P.I. (1985) Fluid evolution in the Notch Peak aureole (abs.). EOS, 66, 389.

Labotka, T.C., Nabelek, P.I., and Papike, J.J. (1988) Fluid infiltration through the Big Horse Limestone Member in the Notch Peak contact-metamorphic aureole, Utah. American Mineralogist, in press.

Laul, J.C. (1979) Neutron activation analyses of geological materials. Atomic Energy Review, 17, 603–695.

Lohmann, K.C. (1977) Causative factors of the outer detrital belt House embayment: A sedimentologic examination of a terrigenous-carbonate depositional system, early Upper Cambrian (Dresbachian), east-central Utah and west-central Nevada. Ph.D. thesis, State University of New York at Stony Brook, Stony Brook, New York.

Morrison, D.M. (1976) Multivariate statistical methods. McGraw-Hill, New York.

Nabelek, P.I., Labotka, T.C., O'Neil, J.R., and Papike, J.J. (1984) Contrasting fluid/rock interaction between the Notch Peak granitic intrusion and argillites and limestones in western Utah: Evidence from stable isotopes and phase assemblages. Contributions to Mineralogy and Petrology, 86, 25–34.

Nabelek, P.I., Papike, J.J., and Laul, J.C. (1986) The Notch Peak granitic stock, Utah: Origin of reverse zoning and petrogenesis. Journal of Petrology, 27, 1035–1069.

Norrish, K., and Hutton, J.T. (1969) An accurate x-ray spectrographic method for the analysis of a wide range of geologic samples. Geochimica et Cosmochimica Acta, 33, 431–453.

SAS (Statistical Analysis System) (1982) SAS user's guide: Statistics. SAS Institute, Cary, North Carolina.

Shaw, D.M. (1956) Geochemistry of pelitic rocks—Part III, major elements and general geochemistry. Geological Society of America Bulletin, 67, 919–934.

Thompson, J.B., Jr. (1959) Local equilibrium in metasomatic processes. In P.H. Abelson, Ed., Researches in geochemistry, p. 427–457. Wiley, New York.

Walther, J.V., and Helgeson, H.C. (1977) Calculation of the thermodynamic properties of aqueous silica and the solubility of quartz and its polymorphs at high pressures and temperatures. American Journal of Science, 277, 1315–1351.